Macromolecular Reaction Engineering
www.mre-journal.de

High Solid Acrylic–Melamine Latexes with Tunable Crosslinking Capability

*Carlos A. Córdoba, Ludmila I. Ronco, Celina E. Barrios, Luis M. Gugliotta, and Roque J. Minari**

Miniemulsion polymerization is employed to produce high solid content (50%) acrylic/melamine latexes with varied crosslinking capability, for their potential application as waterborne crosslinkable coatings. This synthesis strategy allows the efficient incorporation of a hydrophobic crosslinker, iso-butylated melamine (iBMF), into polymer particles, and to obtain latexes with different iBMF concentrations and acrylic polymer with varied content of hydroxylic groups (OH–). The involved crosslinking mechanisms and the physical transformations during film thermosetting of acrylic/iBMF nanocomposite are exhaustively investigated by combining thermal, spectroscopic, and thermo-mechanical analyses. The influence of reactive groups concentration (iBMF and OH– content in the acrylic polymer) on the rate of curing, the crosslinking degree, and consequently onto the sensitive properties of cured films are discussed here.

1. Introduction

The increasing concern for sustainability and the stricter environmental legislation has imposed a trend within the general coatings industry to change from solvent-based formulations to more environmentally friendly options, which contain water as the main solvent (e.g., acrylic latexes). The main challenge of waterborne coatings is to obtain comparable or improved performance of solvent-based formulations with little or no solvent emission. On the other hand, industrial coatings typically have higher performance requirements than those achieved with a thermoplastic latex (like an acrylic latex), which lack hardness, toughness, and solvent resistance.[1] In this scenario, film crosslinking aims to improve the performance of coalesced latex films over the levels attainable with thermoplastic latexes.

Dr. C. A. Córdoba, Dr. L. I. Ronco, Prof. L. M. Gugliotta, Prof. R. J. Minari
Group of Polymers and Polymerization Reactors
Institute of Technological Development for the Chemical Industry (INTEC)
National University of the Litoral - Consejo Nacional de Investigaciones Científicas y Técnicas
Santa Fe 3000, Argentina
E-mail: rjminari@santafe-conicet.gov.ar
Dr. C. E. Barrios
Thermal Analysis Laboratory
Institute of Technological Development for the Chemical Industry (INTEC)
National University of the Litoral - Consejo Nacional de Investigaciones Científicas y Técnicas
Santa Fe 3000, Argentina
The ORCID identification number(s) for the author(s) of this article can be found under https://doi.org/10.1002/mren.201800063.

DOI: 10.1002/mren.201800063

From the early works of Bufkin and Grave,[2–7] crosslinkable latexes have been gaining interest. Crosslinking mechanisms for latexes include the use of crosslinkable agents (or crosslinkers) as well as the autoxidation. The last one involves latexes with allylic functionality, alkyd–acrylic latexes, and the use of small amounts of diene monomers (e.g., butadiene, pentadiene).[8,9] The main disadvantage of this crooslinking strategy is the tendency for films to discolor upon aging (crosslinking) at room temperature. A more widely used approach has been producing reactive latexes by copolymerization of monomers with functional groups such as hydroxyl, carboxyl, or carbonyl (e.g., acrylic acid, hydroxyethyl methacrylate, diacetone acrylamide), and to add an external crosslinker containing amino, epoxy, aziridine, carbodiimides, hydrazide, β-hydroxyalkylamide functionality at the end of the emulsion polymerization.[10–12]

Among the employed crosslinkable agents, melamine formaldehyde (MF) is widely used in industrial coating applications with hydroxyl, carboxyl, and amide functional polymers for producing basecoats and clearcoats.[13,14] One particular strategy employed for producing waterborne crosslinkable formulations, which has been in relatively widespread use over the past decades, involves mixing an acrylic latex with hexamethoxymethyl melamine (HMMM), a water-soluble MF.[10,15–21] The acrylic latex particles are prepared by emulsion polymerization by introducing co-monomers with hydroxyl and carboxylic acid groups that can react upon heating with the alkoxymethyl groups of the MF derivative. Despite water solubility of HMMM facilitates its incorporation in a waterborne acrylic latex, this particular strategy has as a main drawback that homogeneous distribution of crosslinker in formed films are not ensured; and hence films with a non-homogeneous crosslinking density could be obtained. This non-homogeneous crosslinking density is one of the main reasons for the poorer properties obtained with such latexes compared to the solvent-based counterparts, which contain both acrylic and MF dissolved in an adequate solvent.

Miniemulsion polymerization represents an alternative for synthesizing latexes with the efficient compatibilization of a preformed resin in the polymer particles. Miniemulsion polymerization was previously employed for producing alkyd/acrylic,[22,23] polyurethane/acrylic,[24,25] and polybutadiene/polystyrene

nanoparticles.[26] Recently, miniemulsion polymerization was successfully employed for synthesizing 20% solid content acrylic/MF latexes with post-crosslinking capability as an alternative for avoiding face components separation during film formation.[27] This strategy allowed the efficient incorporation of a hydrophobic iBMF into acrylic latex particles.

Film formation by particle coalesce was subject of study for years. It involves the following stages: water evaporation, particle deformation to yield a void-free film, and polymer diffusion across the interparticle boundary.[28] This process is completed when polymer particles are not crosslinked and their T_g is low enough to allow polymer chain diffusion. Thermoset films are obtained by crosslinking reactions which occur by a subsequent heating of coalescing films. The curing mechanisms involved in the crosslinking between the MF crosslinker and the acrylic functional polymer are complex because different crosslinking reactions can simultaneously take place while film physical transformations are induced until reaching the final desired properties.[29,30] MF curing involves the crosslinking reactions between the reactive groups of melamine crosslinker (self-crosslinking) and, more significantly, with hydroxyl and/or carboxylic groups of acrylic polymers (external crosslinking). Curing transitions, such as gelation and vitrification, control a number of properties of the final film, like rheological behavior, reaction rate, hardness, internal stresses, and in fact all structure-related properties of a thermoset film.[31] Therefore, a better understanding of the whole curing process (i.e., involved crosslinking reactions and viscoelastic film transformations) is not only important for optimizing curing conditions of a thermoset system, but it contributes to analyzing the influence of acrylic/MF constituents on final properties of the crosslinked film.

This work investigates the synthesis of high solid (50%) acrylic/iBMF latexes with different crosslinking capabilities. Miniemulsion polymerization is the employed method, and different acrylic/iBMF latexes containing varied content of OH groups and crosslinker are synthesized. Also, an exhaustive study on the curing process of acrylic/iBMF nanocomposite is carried out in order to contribute to the better understanding of i) the involved crosslinking mechanism and ii) the physical transformations during film thermosetting. Finally, the evolution of both the insoluble polymer fraction and the solvent resistance, as sensible properties, are evaluated during the curing process.

2. Experimental Section

2.1. Materials

The following reagents were used as received: hydroxyethyl methacrylate (HEMA, Visiomer Evonik), butyl acrylate (BA, AkzoNobel, technical grade), methyl methacrylate (MMA, Sigma-Aldrich), potassium persulfate (KPS, Mallinckrodt, 99% purity), octadecyl acrylate (OA, Sigma-Aldrich, 97% purity), Dowfax 2EP (Dow, solution containing 45% of active surfactant), hydroquinone (Fluka, <99% purity). The employed iBMF crosslinker provided by INDUR S.A.C.I.F.I. as a 40% xylene solution and contains traces of iso-butanol (iBOH). iBMF was dried under vacuum (5 mmHg) at ambient temperature until constant weight before its use. Tetrahydrofuran (THF, Cicarelli) and methyl ethyl ketone (MEK, Anedra, 99% purity) were used as solvents. Demineralized water was used throughout the work.

2.2. Miniemulsification

The following was common to all miniemulsions: a) 50 wt% of solids; b) 3% wbop (weight based on organic phase) of surfactant (Dowfax 2EP); c) 4% wbm (weight based on monomer) of OA as costabilizer; and d) 0.3% wbw (weight based on water) of $NaHCO_3$.

The acrylic monomeric formulation included BA/MMA (weight ratio: 100/97.6) and different content of OH– functional monomer HEMA (6%, 8%, and 10% wbm). Additionally, variable content of iBMF crosslinker, 10–20% wbm, was employed. Prior to the miniemulsification, iBMF and the costabilizer (OA) were dissolved in the monomer phase, and then mixed with the aqueous phased, containing the surfactant and $NaHCO_3$, by magnetic stirring for 15 min. The resulting preemulsion was sonified for 30 min in a Sonics VC 750 (power 750 watts) at 80% of amplitude, in cycles of 20 s on and 5 s off. This process was carried out in a 100 mL refrigerated jacketed vessel to maintain the miniemulsion temperature below 35 °C.

2.3. Polymerization

Polymerization reactions were carried out in a 0.2 L batch glass reactor equipped with a reflux condenser, a stirrer, a sampling device, and a nitrogen inlet. The reaction temperature (70 °C) was adjusted by manipulation of the reactor jacket temperature, in turn controlled by a water bath. The miniemulsion was loaded into the reactor, and the system was kept under stirring and nitrogen bubbling until the reaction temperature was reached. Polymerizations were started by injecting KPS (0.8% wbm) water solution as a shot. The total polymerization time was 3 h and nitrogen bubbling was maintained during the whole experiment.

2.4. Characterization

2.4.1. Miniemulsion and Latex Characterization

Monomer conversion (x) was determined gravimetrically. Average droplets diameter (d_d) and particles diameter (d_p) were measured by dynamic light scattering (DLS) at a detection angle of 90°, in a Brookhaven BI-9000 AT photometer. Prior to the DLS measurements, the samples were diluted with a water solution saturated with Dowfax 2EP and MMA, in order to avoid droplets destabilization and loss of monomer from droplets and particles. The number of droplets (N_d) and particles (N_p), and their ratio (N_p/N_d) were also calculated from the measurements of x, d_d, and d_p.

The final gel content of latexes, that is, their insoluble fraction, was determined immediately after the polymerization finished,

in order to avoid a possible crosslinking during film formation at room temperature that could affect gel content measurement. It involved directly diluting 0.3 mL of latex in 12 mL of THF during one night and under stirring. Then, the insoluble fraction was separated as a precipitate by centrifugation at 6000 rpm for 2 h. The procedure was repeated onto the precipitate extracted with fresh THF. The final precipitate was dried at 70 °C until constant weight, and the gel fraction was determined by taking into account the solid content and x of the latex.

Particle morphology was determined by TEM, in a JEOL 100 CX (100 kV). Samples of diluted latexes were stained in two steps. First, the diluted latex at 0.01% of solids was treated with 10 µL of 2% of phosphotungstic acid (PTA) solution for 30 min at room temperature to obtain a negative staining of the particle surface. Then, four droplets of the stained diluted latex were placed on copper grids covered with formvar (Fluka), and positively stained with vapors of RuO_4 in a closed vessel for 10 min. RuO_4 reacts with amine groups of iBMF, thus staining MF enriched phase.

2.4.2. Film Characterizations

Polymer films used to measure their properties were prepared by casting the latexes onto silicone right-angled molds at 22 °C and 55% of relative humidity until achieving constant weight. Dried polymer films were carefully peeled from the silicone substrate, obtaining right-angled films, with a final thickness of about 1 mm.

Thermogravimetric analysis (TGA) and differential scanning calorimetry (DSC) were carried out with Q500 and Q2000 equipments from TA Instruments, respectively. For TGA analysis, 5 mg of sample films were heated from 30 to 600 °C with a heating rate of 10 °C min^{-1} under nitrogen atmosphere. Also, in order to simultaneously follow the evolution of the gaseous products generated during the curing process, TGA equipment was connected to a mass spectrometer (TA instruments, Discovery Mass Spectrometer).

DSC measurements were carried out with a heating ramp at 10 °C min^{-1} from –60 to 220 °C, using 5 mg of sample films placed in a TZero hermetic aluminum sample pan.

Dynamic mechanical thermal analysis (DMTA) was employed to follow the curing process and physical transformations of acrylic/iBMF films. To this effect, films of 1 mm thick was analyzed by using the single cantilever-bending mode at a frequency of 1 Hz between 30 and 300 °C at a heating rate of 5 °C min^{-1}, using a Q800 DMA equipment from TA Instruments.

The film insoluble fraction (FIF) after curing was determined by Soxhlet extraction with THF for 24 h. Also, film resistance to organic solvent was evaluated by immersing 6 mm diameter film samples in MEK at room temperature. The relative mass absorbed was calculated after 14 days of immersion.

3. Results and Discussion

In the present work, we explore the synthesis of acrylic/iBMF latexes with high solid content (50%) by miniemulsion polymerization. Acrylic/iBMF latexes with variable content of crosslinker (iBMF) and concentration of hydroxylate-functional monomer (HEMA) in the acrylic polymer were synthesized, in order to control the crosslinking capability during the films curing. The experimental codes contains the abbreviations ''M'' for iBMF and "H" for HEMA followed by a subscript indicating their concentrations expressed in % wbm. Thus, $M_{15}H_8$ refers to a sample synthesized with concentrations of iBMF and HEMA of 15% and 8% wbm, respectively.

Table 1. Global polymerization results and latex gel content.

Exp.	x [%]	d_p [nm]	N_p/N_d	Gel [%]
$M_{10}H_8$	97	121	1.2	3.5
$M_{15}H_8$	95	134	1.0	5.0
$M_{20}H_8$	95	124	1.3	2.7
$M_{15}H_6$	96	134	1.0	2.9
$M_{15}H_{10}$	95	125	1.0	4.5

3.1. Synthesis of Acrylic/MF Latexes

Table 1 summarizes the global polymerization results and gel content, while the evolution of x and d_p along polymerization reactions are shown in Figure S1, Supporting Information. Independently of the organic phase composition (variable concentrations of iBMF and HEMA), high final x (≥95%) and similar polymerization rate were achieved in all experiments. Additionally, final N_p/N_d ratio is close to unity (Table 1) and d_p remains almost constant along the polymerizations (Figure S1, Supporting Information), indicating that particles were mainly formed by droplets' nucleation. This mechanism of particle formation allowed that the dissolved preformed crosslinker (iBMF) in the droplets remained incorporated in the polymer particles. **Figure 1** shows the TEM picture of sample $M_{15}H_8$, where it can be observed that most particles contain a rich iBMF phase (the stained phase), evidencing their formation by droplet nucleation and the efficient incorporation of MF crosslinker into polymer

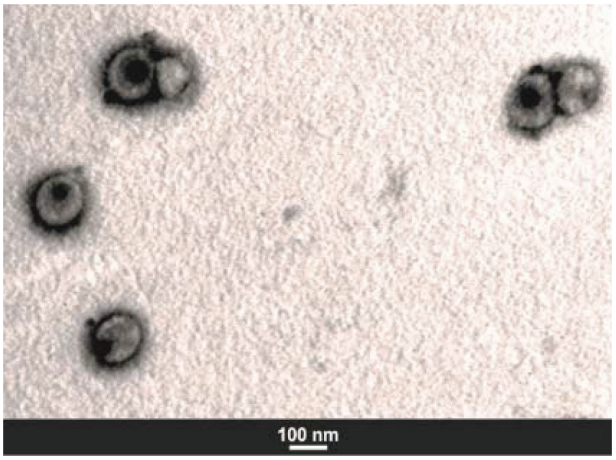

Figure 1. TEM micrography of the acrylic/iBMF particles in the final latex $M_{15}H_8$.

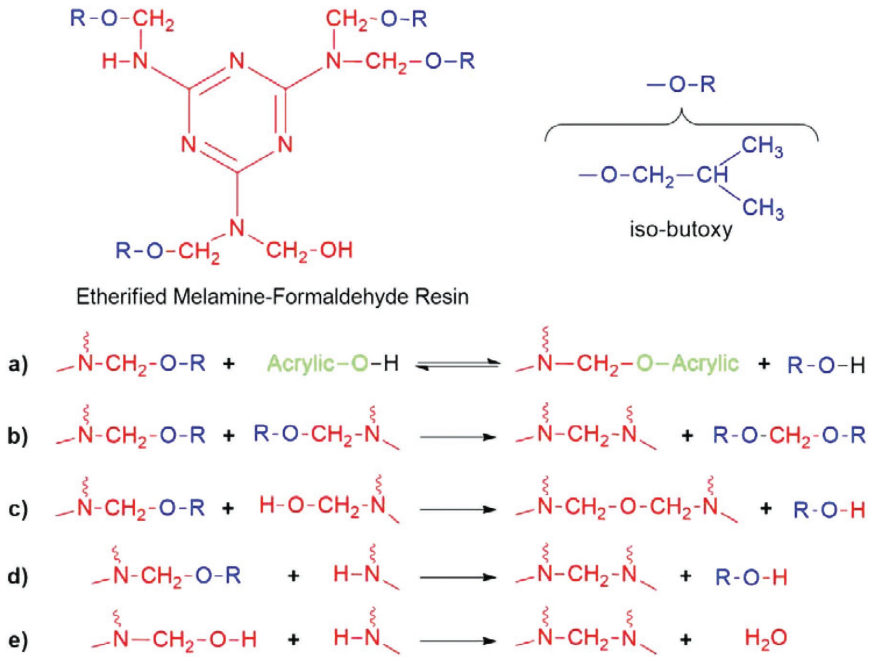

Figure 2. Crosslinking reactions involving iBMF and an OH-functionalized acrylic.

particles with an almost homogeneous content. Moreover, the insignificant contribution of homogeneous nucleation is an evidence that polymerization in aqueous phase was not important and it was not affected by the range used for HEMA concentration.[32] This observation was also corroborated by analyzing the fraction and composition of solids presented in aqueous phase (see Table S1 and Figure S2, Supporting Information).

Synthesized latexes present a small fraction of insoluble polymer (gel), which are in agreement with that values reported for the BA/MMA emulsion copolymerization with similar acrylic composition.[33] It is well known that PBA can suffer intra-/inter-molecular chain transfer to the polymer forming gel by termination combination.[34] These results indicate that crosslinking reactions between iBMF and acrylic polymer do not happen during polymerization, thus latexes conserve the crosslinking capability until the formation of films and their curing treatment at high temperature.

3.2. Crosslinking Process

According to iBMF technical specification and its spectroscopy characterization, the MF crosslinker used in this work corresponds to a highly iBMF, with the following average reactive group composition: 75 mol% of iso-butoxy, 24 mol% of methylol and 1 mol% of imino groups. For this highly alkylated melamine, the desired crosslinking reaction between the OH– of acrylic polymer and iso-butoxy groups of iBMF involves an ether crosslinking and the release of iBOH (**Figure 2**, reaction a).[35] However, self-crosslinking reactions among reactive iBMF groups, iso-butoxy, methylol, and imino groups, could also be present (Figure 2, reactions b–e). It could be expected that reactions d and e are less probable than those of b and c, due to the low concentration of imino groups in this highly alkylated MF crosslinker. Self-crosslinking reactions could be present during cure of acrylic/iBMF films since all latex formulations contain an excess of MF iso-butoxy groups with respect to OH– groups of acrylic polymer (Table S2, Supporting Information).

3.2.1. TGA and Mass Spectroscopy

TGA analysis onto acrylic/iBMF films was conducted in order to associate mass losses with crosslinking reactions and film thermal degradation. **Figure 3** shows the TGA thermograms of all synthesized samples with different concentrations of HEMA and iBMF. It can be observed a small weight loss in the temperature range of 130–250 °C, which could be associated with the evaporation of crosslinking products, followed by the main weight loss event assigned to the thermal degradation of the material. Similarly, the TGA thermogram of pure iBMF also presents two weight loss events in the temperature range of 130–350 °C and 350–430 °C, respectively (Figure S3, Supporting Information). The first weight loss was attributed to the formation of volatile products by self-crosslinking reactions, while the second weight loss event was assigned to the thermal degradation of the material.[36]

Moreover, most of the acrylic/iBMF synthesized samples showed a considerable thermal resistance up to approximately 250 °C, which implies a safer application of these cured coatings up to the given temperature. However, sample $M_{20}H_8$ presents the highest thermal resistance (degradation was considerably above 330 °C) probably as a consequence of a high contribution of iBMF self-crosslinking. Note that self-crosslinking on pure iBMF produced a material with higher thermal resistance

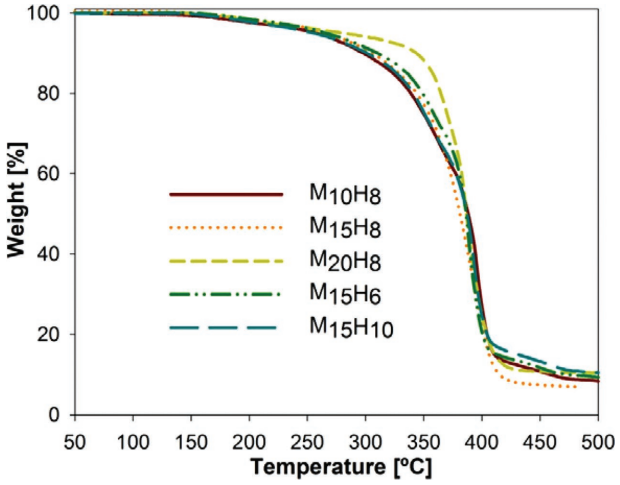

Figure 3. TGA thermograms for the obtained acrylic/iBMF films.

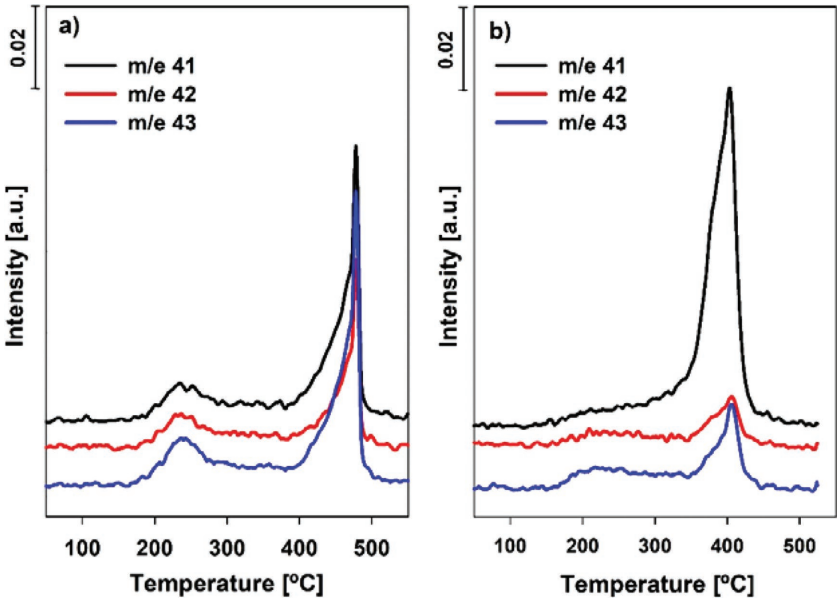

Figure 4. Mass spectroscopy (MS) signals for iBOH main fragments during the TGA of a) pure iBMF and b) $M_{15}H_8$.

(approximately 350 °C, Figure S3, Supporting Information) than acrylic/iBMF films.

Additionally, mass spectra of the gaseous components produced during TGA experiments were recorded in order to increase the knowledge of the curing process. All ranges of mass-to-charge signals (m/z = 1–76) was recorded. **Figure 4** shows the evolution of signals m/z = 41, m/z = 42, m/z = 43, attributed to the principal fragmentations of iBOH (1-propanol, 2-methyl)[37] during TGA experiments of pure iBMF and $M_{15}H_8$ sample. No other species could be clearly distinguished in the mass spectra.

During TGA-MS experiments of both pure iBMF and $M_{15}H_8$ samples, the presence of iBOH in the gas phase was observed in the temperature range of 150–270 °C, corresponding to the curing process according to the weight loss observed in TGA thermograms (Figure 3 and Figure S3, Supporting Information). Moreover, the signals attributed to water (m/z = 18) and diisobutoxymethane (main fragment m/z = 57) release were absent, indicating that iBMF self-crosslinking reactions b and e (Figure 2) were negligible. From the TGA-MS experiment of pure iBMF, it could be concluded that self-crosslinking of iBMF mainly involves iBOH release, mainly as a contribution of reaction c since the very low imino groups content of iBMF limits the occurrence of reaction d (Figure 2).

On the other hand, release of iBOH during curing of sample $M_{15}H_8$ was attributed to the desired crosslinking reaction between the –OH of acrylic polymer and iso-butoxy groups of iBMF (Figure 2, reaction a). Nevertheless, self-crosslinking of iBMF (reaction c) could take place, but it was not possible to distinguish between them since iBOH is released in both cases. Note that weight loss in the temperature range of 130–250 °C for $M_{15}H_8$ (Figure 3) was smaller than that observed for iBMF (Figure S3, Supporting Information), and consequently lower MS signals were detected for the acrylic/melamine sample. Finally, both samples showed a significant peak in the acquired MS signals, which corresponded to the main weight loss by thermal degradation (above 300 °C).

3.2.2. Differential Scanning Calorimetric Analysis

DSC was used to further investigate the curing process of the obtained acrylic/iBMF films. **Figure 5** shows the exothermic curing peak obtained during DSC for sample $M_{15}H_{10}$ and the corresponding TGA thermogram in the same temperature range. Correlation between both thermal analyses confirms that the observed weight loss in TGA is associated to the exothermic curing process. **Table 2** summarizes the main curing process characteristics determined from DSC analysis: the temperature range where the curing peak is observed (ΔT_{cur}), the temperature corresponding to the curing peak maximum (T_{max}), and the heat of curing reactions (ΔH_{cur}). Also, weight loss percent in the temperature range of the curing peak determined by TGA (WL_{cur}) is included in Table 2. It is worth mentioning that WL_{cur} results are in agreement with the theoretical weight loss values of iBOH release by crosslinking occurrence according to reactions of Figure 2. Taking as example sample $M_{15}H_8$, the complete consumption of OH– groups of acrylic polymer, through the desired reaction with iBMF (i.e., only external crosslinking), would produce a weight loss of 4% due to iBOH release. For the other samples, the examination of TGA and

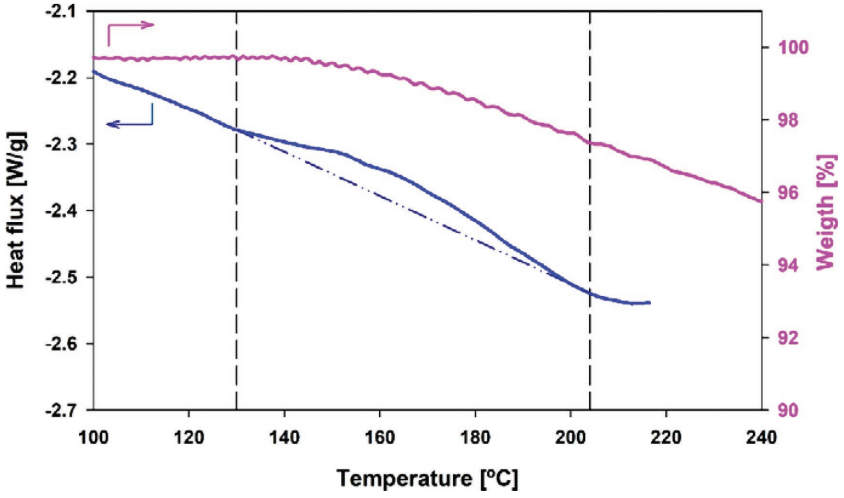

Figure 5. DSC and TGA thermograms of $M_{15}H_{10}$ sample in the range of temperature where curing occurs.

Table 2. Main results of the curing study for acrylic/melamine films using DSC and TGA.

Film	DSC			TGA
	ΔT_{cur} [°C]	T_{cmax} [°C]	ΔH_{cur} [J g^{-1}]	WL_{cur} [%]
$M_{10}H_8$	130–205	161.9	0.71	2.15
$M_{15}H_8$	130–210	167.9	0.96	2.19
$M_{20}H_8$	128–207	167.1	2.19	2.12
$M_{15}H_6$	142–196	166.1	0.28	1.37
$M_{15}H_{10}$	130–204	164.4	1.30	2.37

DSC thermograms reveals that these acrylic/melamine films can be safely cured in the temperature range of 130–210 °C with a T_{cmax} around 162–168 °C (Table 2).

The increment in concentrations of iBMF or HEMA generates higher ΔH_{cur} (Table 2), which was associated to a higher crosslinking degree. During cure of sample $M_{15}H_6$, with the lowest concentration of OH– in acrylic polymer, the lowest values of both ΔH_{cur} and WL_{cur} were observed. Additionally, the higher ΔH_{cur} values were observed for films containing the higher concentrations of the reactive groups, $M_{20}H_8$ and $M_{15}H_{10}$.

3.2.3. Dynamic Mechanical Thermal Analysis

Additionally, the curing process was followed by DMTA, which is a sensitive method for measuring the evolution of the rheological material functions of a polymer as crosslinking proceeds. DMTA analysis started at 30 °C just above the T_g of uncrosslinking polymer determined by DSC (Table S3, Supporting Information).

Figure 6 presents the evolution of storage modulus (E'), the loss modulus (E''), and the loss factor, tan δ, during DMTA assays. At the beginning of the DMTA analysis, films are in an uncrosslinked rubber state. As temperature increases, E' and E'' go down and a first cross point is shown at approximately 50 °C, from which materials acquired a higher viscous behavior ($E'' > E'$). Around 110–120 °C ($T_{E',min}$), E' reaches a minimum value (E'_{min}, **Table 3**) followed by a progressive increment, as indication of crosslinking process starts.[38] Moreover, the temperatures values determined by DMTA are in agreement with the beginning of curing process observed by DSC.

The increase in molecular weight by crosslinking reactions induces gelation, which is characterized by the increase in molecular weight and the formation of a crosslinked network. During this transition state, from a more viscous material

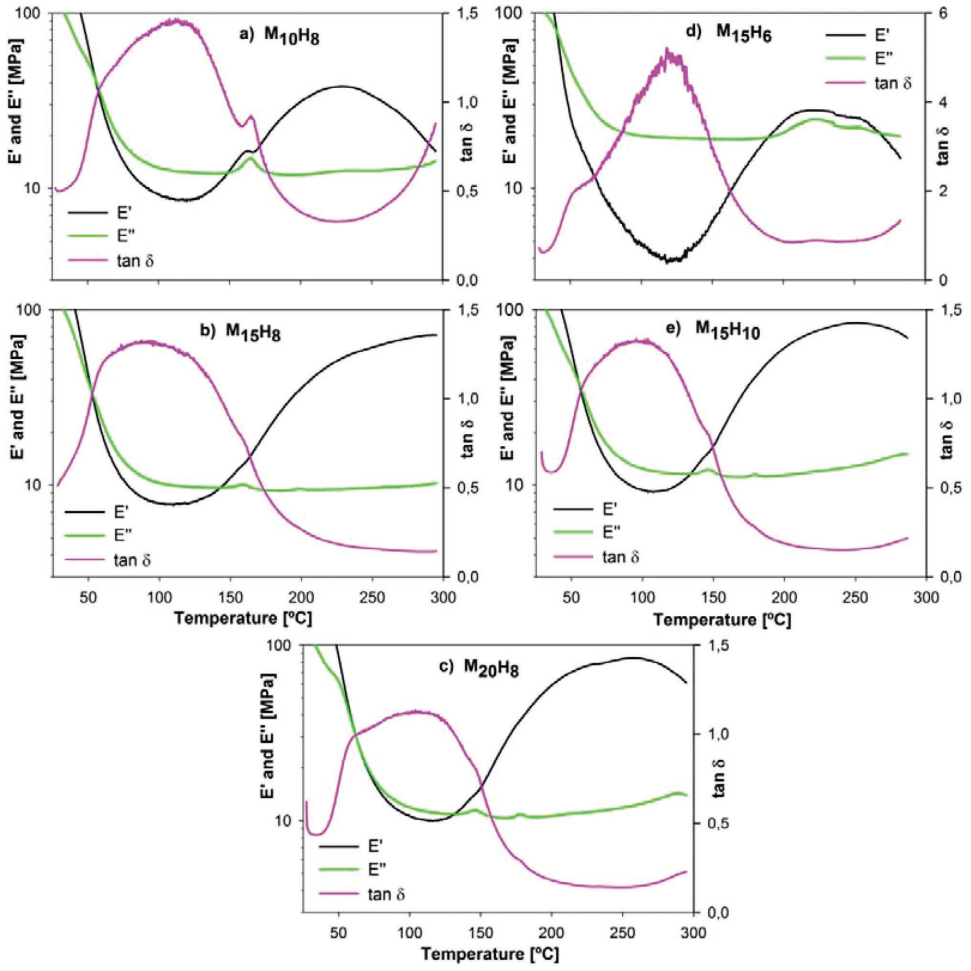

Figure 6. Evolution of E' and E'' as crosslinking proceeds for films a) $M_{10}H_8$, b) $M_{15}H_8$, c) $M_{20}H_8$, d) $M_{15}H_6$, and e) $M_{15}H_{10}$.

Table 3. Main results of the curing study of acrylic/melamine films using DMTA.

Exp.	$T_{E',min}$ [°C]	E'_{min} [MPa]	T_{gel} [°C]	$T_{E',min}$ [°C]	E'_{max} [MPa]	$\Delta E'$ [MPa]	Tv_1 [°C]	T_{v2} [°C]
$M_{10}H_8$	120	8.5	149	230	38.2	29.7	165	233
$M_{15}H_8$	110	7.7	143	292	71.7	64.0	161	198
$M_{20}H_8$	114	10.0	132	257	84.4	74.4	146	178
$M_{15}H_6$	118	3.7	189	223	28.0	24.3	223	—
$M_{15}H_{10}$	104	9.1	134	251	84.0	74.9	147	179

(tan $\delta > 1$) to a solid (tan $\delta < 1$), tan δ would be expected to be equal to 1, and the temperature at which a resin starts gelling, the "gel point," would be estimated by the cross-over point of the two modulus curves ($E' = E''$).[38,39] However, this is only an approximate gel point, because it has been demonstrated that frequency-dependent measurements are required, since tan δ is frequency independent at the gel point.[40,41] Irreversible gel formation was evident for all films samples, but the gel point happened at lower temperature (lower time) for film with higher concentration of iBMF and/or HEMA (T_{gel}, Table 3).

After gel point, E'' exhibits a first peak (Figure 6), which was identified as a first vitrification point, that is, the rubber-to-glass transition (T_g) of the partially cured material. Vitrification occurs when the reaction rate is faster than the heating rate, allowing the T_g of partially cured polymer reaches the experimental temperature.[38] The vitrification point gives information about the rate of curing, because it describes the transition temperature of the crosslinked network during the curing process.[42] When the experimental temperature increases above this first observed vitrification point, crosslinking even proceeds and the T_g of the partially cured polymer could also increase. Therefore, under such condition, E'' could exhibit a second peak, which is evidenced in most of the analyzed samples, indicating a second vitrification point. An amplification of E'' evolution with temperature for all analyzed samples are presented in **Figure 7**.

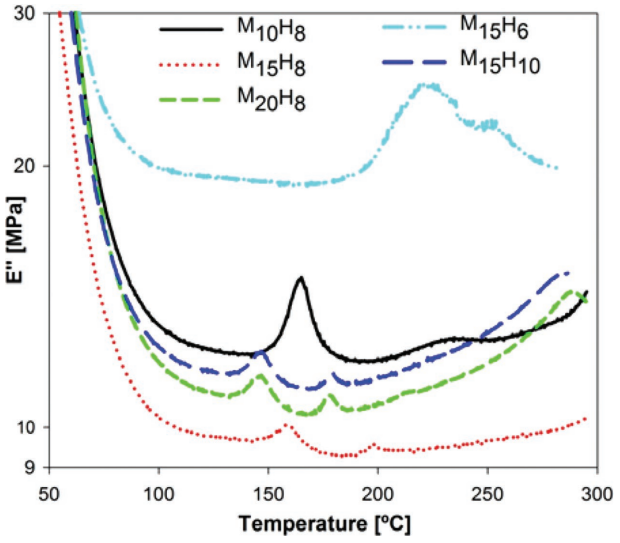

Figure 7. Vitrification temperatures observed in the evolution of E'' during DMTA analysis.

Sample vitrification temperatures are indicated as T_{v1} and T_{v2} in Table 3. These transitions were also observed, at the same temperature, in tan δ as shoulders or peaks (Figure 6).

The concentration of both reactive components has a significant influence on crosslinking rate. An increase in the concentration of both reactive components, HEMA and iBMF, promoted a faster crosslinking rate, that is, first vitrification point happened at lower temperatures (T_{V1} = 146–147 °C). The reduction on the concentration of HEMA in the acrylic polymer from 10% to 6% (at constant content of iBMF = 15%, $M_{15}H_{10}$ and $M_{15}H_6$ samples) generates an important increase in the first vitrification temperature from 147 °C to 223 °C. Also, the lowest content of HEMA in $M_{15}H_6$ sample does not only present a low crosslinking rate, but also shows one single wide vitrification peak. Also note that in this sample the evolution of E' shows the lowest values before curing turns predominant. Probably, the lowest concentration of OH– groups in the acrylic chain of this sample reduced the probability of early curing and E' is further reduced due to a higher contribution of polymer softening during heating. On the contrary, crosslinking rate of films is not significantly degraded by varying the iBMF concentration, while maintaining the HEMA content of acrylic polymer (T_{v1} changes from 146 to 165 °C). These last results are evidence that the OH– content of acrylic polymer had a stronger influence on the rate of formation of a crosslinking network than iBMF concentration. Therefore, external crosslinking reactions (i.e., the generation of acrylic–iBMF crosslinks) have a more significant contribution than iBMF self-crosslinking (i.e., generation of iBMF–iBMF crosslinks) onto the formation of the acrylic/MF crosslinked structure.

Crosslinking reaction still took place after vitrification, indicating that this transition does not correspond to the glass transition of fully crosslinked network ($T_{g\infty}$). However, the further increase in T_g of the partially cured polymer at higher temperatures reduces the mobility in the material and retards crosslinking, which was observed as a slowing down of E' growth, until reaching its maximum value at 223–292 °C ($T_{E'max}$ and E'_{max}, Table 3). Crosslinking completion under such a condition is considered a diffusion controlled curing process. Films show a decrease in E' at temperatures higher than those corresponding to E'_{max}. This could be a consequence of reaching the film degradation temperature (around 250 °C according to TGA measurements), generating the loss of crosslinked network identity. The difference between E'_{max} and E'_{min}, called $\Delta E'$ in Table 3, could be used as an indication of the cured film rigidity and its crosslinking degree.[43] As was expected, higher concentration of reactive compounds

Table 4. Solvent resistance (MEK absorption) of melamine-containing films before curing (BC) and after curing at 150 °C for 3 h (AC), after 14 days of immersion.

Film	MEK absorption [%]	
	BC	AC
$M_{10}H_8$	1991	124
$M_{20}H_8$	1656	103
$M_{15}H_6$	3390	145
$M_{15}H_{10}$	1347	106

(iBMF or HEMA) resulted in films with higher crosslinking degree (i.e., higher $\Delta E'$).

3.2.4. Solvent Resistance of Film

As further evidence of curing, it was observed that the insoluble fraction in cured films reaches values close to 100% (see Table S4, Supporting Information, FIF values reached after curing), compared to the low latex gel content which was around 5%.

Additionally, results of films resistance to MEK (measured as percentage of MEK absorption) before (BC) and after (AC) curing post-treatment are shown in **Table 4**. It is expected that solvent resistance of films, measured as the relative mass absorbed, must be strongly influenced by the degree of crosslinking. Before curing, films resisted MEK assays (i.e., 14 days of immersion in MEK), but with a very high level of MEK absorption (higher than 1500%). However, after curing, the presence of crosslinking in the acrylic/iBMF matrix significantly improved the solvent resistance, reducing MEK absorption after 14 days of immersion to around 100%. These results are in accordance with the FIF values obtained. In particular, cured films with higher concentration of HEMA and/or iBMF, presented lower MEK absorption values due to the higher crosslinking degree.

4. Conclusions

Acrylic/iBMF nanocomposites with crosslinking capability were synthesized through high solid miniemulsion polymerization. Latexes with droplet nucleation as the main mechanisms of particles formation were produced, which ensured the efficient incorporation of variable content of iBMF crosslinker into acrylic particles.

By combining DSC, TGA-MS, and DMTA results, the main crosslinking mechanisms and physical transformations during film thermosetting were identified. These analyses revealed that crosslinking reactions took place when films were exposed at a temperature range of 130–210 °C, generating iBOH as main crosslinking product. iBOH formation was attributed to the desired crosslinking reaction between the OH– of acrylic polymer and iso-butoxy groups of iBMF, and to the self-crosslinking reaction between iso-butoxy groups and methylol groups of iBMF molecules. The rheological characterization during film curing could be used to determine how concentration of reactive groups in the acrylic/iBMF films influenced crosslinking kinetic and film transformations. While crosslinking degree was influenced by the content of both reactive components (OH– and iBMF), curing rate and films transitions (such as gelation and vitrification) were mainly governed by the OH– content of acrylic polymer. In this context, a film more resistant to solvent and with improved mechanical properties is reached when using the highest concentration of both reactive components (HEMA and iBMF), while a fast thermal-curing film is obtained by increasing HEMA acrylic content.

Finally, this work demonstrates that miniemulsion polymerization is a promising process to obtain waterborne acrylic/melamine latexes with high solid content and tunable crosslinking capability, for their potential application as crosslinkable coatings.

Supporting Information

Supporting Information is available from the Wiley Online Library or from the author.

Acknowledgements

The financial support received from CONICET, UNL, and ANPCyT (all of Argentina) is gratefully acknowledged. The authors also thank INDUR S.A.C.I.F.I. for providing the iBMF crosslinker employed.

Conflict of Interest

The authors declare no conflict of interest.

Keywords

miniemulsion polymerization, thermal crosslinking, waterborne acrylic/melamine latex

Received: September 21, 2018
Revised: November 18, 2018
Published online:

[1] V. Nemanič, B. Zajec, M. Žumer, N. Figar, M. Kavšek, I. Mihelič, *Appl. Energy* **2014**, *114*, 320.
[2] B. G. Bufkin, J. R. Grawe, *J. Coat. Technol.* **1978**, *50*, 41.
[3] J. R. Grawe, B. G. Bufkin, *J. Coat. Technol.* **1978**, *50*, 67.
[4] B. G. Bufkin, J. R. Grawe, *J. Coat. Technol.* **1978**, *50*, 83.
[5] J. R. Grawe, B. G. Bufkin, *J. Coat. Technol.* **1978**, *50*, 70.
[6] B. G. Bufkin, J. R. Grawe, *J. Coat. Technol.* **1978**, *50*, 65.
[7] J. R. Grawe, B. G. Bufkin, *J. Coat. Technol.* **1979**, *51*, 34.
[8] V. D. Athawale, R. V. Nimbalkar, *J. Am. Oil Chem. Soc.* **2011**, *88*, 159.
[9] Z. W. Wicks Jr, F. N. Jones, P. Pappas, D. A. Wicks, *Organic Coatings: Science and Technology*. Wiley, Hoboken, NJ **2007**.
[10] L. S. Tang, M. Zhang, S. F. Zhang, J. Z. Yang, *Prog. Org. Coat.* **2004**, *49*, 54.
[11] J. W. Taylor, M. A. Winnik, *J. Coat. Technol. Res.* **2004**, *1*, 163.
[12] A. Ruckerova, J. Machotova, R. Svoboda, K. Pukova, P. Bohacik, R. Valka, *Prog. Org. Coat.* **2018**, *119*, 91.
[13] S. M. Magami, J. T. Guthrie, *Surf. Coat. Int.* **2016**, *95*, 64.

[14] M. R. L. Paine, N. A. Pianegonda, T. T. Huynh, M. Manefield, S. A. MacLaughlin, S. A. Rice, P. J. Barker, S. J. Blanksby, *Prog. Org. Coat.* **2016**, *99*, 330.
[15] M. D. Soucek, E. P. Pedraza, *J. Coat. Technol. Res.* **2009**, *6*, 27.
[16] S. Bas, M. D. Soucek, *React. Funct. Polym.* **2013**, *73*, 291.
[17] M. A. Winnik, P. Pinenq, C. Krüger, J. Zhang, P. V. Yaneff, *J. Coat. Technol.* **1999**, *71*, 47.
[18] R. Ravichandran, J. Florio, *Eur. Coatings J.* **2013**, *6*, 26.
[19] L. T. W. Lin, K. J. Wu, K. Inagaki, J. Billiani, *US Patent 9 796805*, **2017**.
[20] F. Yu, Y. Fang, J. Wang, Y. Xu, J. Shi, *Colloid Polym. Sci.* **2016**, *294*, 1359.
[21] J. P. S. Farinha, S. Piçarra, C. Baleizão, J. M. G. Martinho, in *Industrial Applications for Intelligent Polymers and Coatings* (Eds: M. Hosseini, A. S. H. Makhlouf) Cham, Switzerland **2016**, Ch. 29.
[22] R. J. Minari, M. Goikoetxea, I. Beristain, M. Paulis, M. J. Barandiaran, J. M. Asua, *Polymer* **2009**, *50*, 5892.
[23] R. Udagama, C. de las Heras Alarcón, J. L. Keddie, J. G. Tsavalas, E. Bourgeat-Lami, T. F. L. Mckenna, *Macromol. React. Eng.* **2014**, *8*, 622.
[24] A. Lopez, E. Degrandi-Contraires, E. Canetta, C. Creton, J. L. Keddie, J. M. Asua, *Langmuir* **2011**, *27*, 3878.
[25] N. Ballard, P. Carretero, J. M. Asua, *Macromol. React. Eng.* **2013**, *7*, 504.
[26] L. I. Ronco, R. J. Minari, L. M. Gugliotta, *Macromol. React. Eng.* **2016**, *10*, 29.
[27] C. A. Córdoba, S. E. Collins, M. C. G. Passeggi Jr, S. E. Vaillard, L. M. Gugliotta, R. J. Minari, *Prog. Org. Coat.* **2018**, *118*, 82.
[28] J. L. Keddie, *Mater. Sci. Eng. R Rep.* **1997**, *21*, 101.
[29] A. M. Natu, M. R. Van De Mark, *Prog. Org. Coat.* **2015**, *81*, 35.
[30] Y. Huang, F. N. Jones, *Prog. Org. Coat.* **1996**, *28*, 133.
[31] P. O. Hagstrand, C. Klason, L. Svensson, S. Lundmark, *Polym. Eng. Sci.* **1999**, *39*, 2019.
[32] C. S. Chern, J. C. Sheu, *J. Polym. Sci., Part A: Polym. Chem.* **2000**, *38*, 3188.
[33] I. González, J. M. Asua, J. R. Leiza, *Polymer* **2007**, *48*, 2542.
[34] C. Plessis, G. Arzamendi, J. R. Leiza, H. Schoonbrood, D. Charmot, J. M. Asua, *Macromolecules* **2000**, *33*, 9786.
[35] D. R. Bauer, *Prog. Org. Coat.* **1986**, *14*, 193.
[36] D. J. Merline, S. Vukusic, A. A. Abdala, *Polym. J.* **2013**, *45*, 413.
[37] NIST Chemistry WebBook, https://webbook.nist.gov/chemistry// (accessed: September **2018)**.
[38] R. P. Chartoff, J. D. Menczel, S. H. Dillman, in *Thermal Analysis of Polymers: Fundamentals and Applications* (Eds: J. Mencze, R. Bruce Prime) New Jersey **2009**, Ch. 5.
[39] C.-Y. M. Tung, P. J. Dynes, *J. Appl. Polym. Sci.* **1982**, *27*, 569.
[40] W. Stark, *Polym. Test.* **2013**, *32*, 231.
[41] W. Stark, M. Jaunich, J. McHugh, *Polym. Test.* **2015**, *41*, 140.
[42] X. Cai, B. Riedl, H. Wan, S. Y. Zhang, X.-M. Wang, *Composites, Part A* **2010**, *41*, 604.
[43] S. Kim, H. J. Kim, *Thermochim. Acta* **2006**, *444*, 134.

